

# Development of Immunity Test System with Pseudo Bio-Signal Generator for Wearable Devices and Application to ESD Test of Artificial Hand

Jianqing Wang, *Member, IEEE*, Ryo Nakaya, Keisuke Sato, Daisuke Anzai, *Member, IEEE*, Osamu Fujiwara, *Life member, IEEE*, and Fujio Amemiya, *Member, IEEE*

**Abstract**—In this study, we developed an immunity test system for wearable devices used for healthcare or assistance to people with disabilities. The immunity test system consists of a pseudo bio-signal generator for generating various vital signals such as electrocardiogram (ECG) or electromyography (EMG), and a bio-equivalent gel phantom for simulating a part of the human body. As an application to the electrostatic discharge (ESD) immunity test for a myoelectric artificial hand, we used the pseudo bio-signal generator to generate various myoelectric signals, and confirmed a high correlation between the generated and the real myoelectric signals. We then applied this system to the IEC61000-4-2 specified ESD test. Through a comparison between the ESD test results by using the immunity test system and the result for a real human body, we found a high similarity between them, which suggests that the proposed immunity test system is feasible for various immunity tests in wearable devices.

**Index Terms**—Wearable device, immunity test, ESD, myoelectric artificial hand, bio-signal generator.

## I. INTRODUCTION

Along with the progress of an aging society, wearable devices for collecting and monitoring bio-signals and for application to healthcare and medical fields are beginning to spread [1]-[4]. However, the deterioration of the electromagnetic environment is conspicuous; hence, the electromagnetic interference on wearable devices, caused by various electromagnetic radiations as well as electrostatic discharge (ESD), cannot be ignored [5]-[8]. Wearable devices used in healthcare and medical fields are required to have high immunity performance against electromagnetic disturbances to prevent malfunction during daily life. Therefore, testing whether wearable devices have sufficient immunity performance even under the influence of external electromagnetic fields is necessary. Some wearable devices, for example, wearable electrocardiogram (ECG) or electromyography (EMG), are usually used to detect bio-signals on the human body. This means that the wearable device is essential to the existence of the human body. The human body not only provides the bio-signals constantly to the wearable device to function, but also determines the interference level on the wearable device, which is caused

by the coupling between the human body and external electromagnetic fields. Moreover, as reported in [5], when the human body with a wearable device is electrically charged or discharged, the electric potential abruptly changes. As a result, the wearable device may be exposed, in close proximity, to the resultant transient electromagnetic field, which can also cause malfunctions in the device. Therefore, the ESD immunity test method for wearable devices needs different specifications from other conventional test methods, but this is not yet considered in the current international standards [9]. In February 2017, we submitted a document to a working group of the International Electrotechnical Commission (IEC) - International Special Committee on Radio Interference (CISPR), and initialized a discussion on methods to test the immunity of a wearable robotic equipment at CISPR/I/WG4 [10]. As a result of deliberation at the IEC Advisory Committee on Electromagnetic Compatibility, the Technical Committee TC62/SC62D in charge of medical electronic devices is being advised to investigate the possible immunity methods, because wearable devices can be used for healthcare or medical applications. For the immunity test of wearable devices, continuously producing a stable bio-signal from the human body during the entire immunity testing period is difficult. The individual difference of bio-signals also adversely affects the reproducibility of immunity test results. From these points of view, conducting an immunity test with real human beings is not realistic.

In this paper, we propose an immunity test system for wearable devices by combining a pseudo bio-signal generator and a bio-equivalent gel phantom. First, we describe the constitution of the pseudo bio-signal generator and the test system. Then as an example, we apply the developed immunity test system to perform an indirect ESD immunity test for a myoelectric artificial hand. By actually carrying out an operational test of the myoelectric artificial hand using the developed immunity test system in compliance with the IEC 61000-4-2 ESD immunity testing method [9], we compare the tendency of the malfunction rate in the developed test system with that in a real human body, and demonstrate the test system's validity.

This paper is organized as follows. Chapter II describes the proposed immunity test system consisting of a pseudo bio-signal generator and a bio-equivalent gel phantom. Chapter III describes its application to the indirect ESD test of a myoelectric artificial hand for demonstrating the test system's validity. Chapter IV concludes this paper.

J. Wang, R. Nakaya, K. Sato, D. Anzai, and O. Fujiwara are with the Graduate School of Engineering, Nagoya Institute of Technology, Gokiso-cho, Showa-ku, Nagoya 466-8555, Japan. e-mail: wang@nitech.ac.jp

F. Amemiya is with The University of Electro-Communications, Chofu-shi, Tokyo 182-8585, Japan.

Manuscript received \*, 201x; revised \*, 201x.

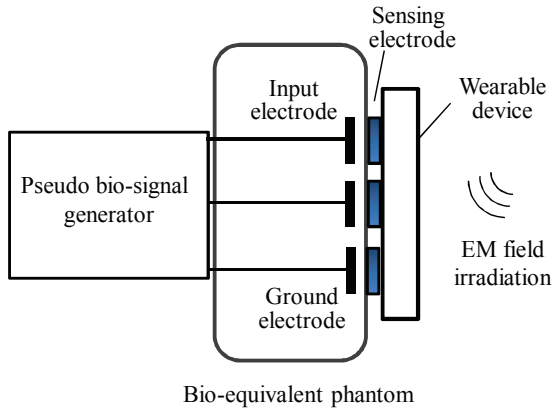


Fig. 1. Configuration of immunity test system.

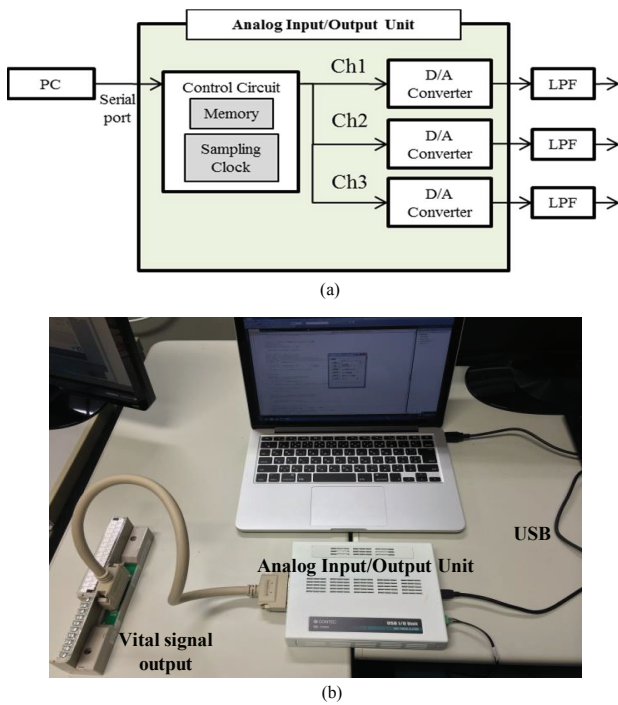


Fig. 2. Pseudo bio-signal generator. (a) Block diagram. (b) Actual view.

## II. IMMUNITY TEST SYSTEM

Figure 1 shows the configuration of the immunity test system, which consists of a pseudo bio-signal generator for generating various bio-signals and a bio-equivalent phantom for simulating a part of the human body.

### A. Pseudo Bio-Signal Generator

When constructing an immunity test system for a wearable device, since the bio-signal is obtained from the human body, it is difficult to keep the bio-signal reproducible and stably maintained during the entire testing period, due to fatigue and individual differences of human subjects. These problems may affect the reproducibility of the immunity test results, and make the reliability of the test results uncertain. Hence, using a signal generator that continuously outputs stable signals on

TABLE I  
RECIPE FOR MAKING THE BIO-EQUIVALENT PHANTOM

Glycerin	300.0 g
Deionized water	417.9 g
Sodium benzoate	2.1 g
Agar	21.6 g

behalf of a human body is desirable. Therefore, we developed a pseudo bio-signal generator capable of mechanically outputting a bio-signal acquired from the human body in advance.

Figure 2 shows the block diagram of a newly developed pseudo bio-signal generator and its photograph. The pseudo bio-signal generator is composed of a personal computer (PC), a microprocessor-based control circuit, and three digital/analog (D/A) converters and low-pass filters. In the pseudo bio-signal generator, the actual bio-signals acquired in advance from a human body are saved as digital data sampled at a specified rate on the PC. According to the requirement of output, the bio-signal data are sent to the analog input/output unit from the PC, and then are divided into different output channels by the control circuit. The digital data are subsequently converted and smoothed into analog bio-signals by the D/A converters and low-pass filters. The analog input/output unit employs a commercially available device (CONTEC: AO-1604LX-USB) with 16-bit resolution and outputs analog signals in the range of  $\pm 10$  V that can be used as pseudo bio-signals required for performing the immunity test of wearable devices.

### B. Bio-Equivalent Gel Phantom

Since a wearable device is expected to acquire bio-signals on the human body by using conducting electrodes, simulating the bio-signal acquisition on the human body is necessary. For this purpose, a pair of signal input electrodes are embedded inside the bio-equivalent phantom, and a bio-signal from the pseudo bio-signal generator is added to the input electrodes for simulating a bio-signal in the human body. The bio-equivalent phantom is a gel-like phantom composed of glycerin, deionized water, sodium benzoate, and agar [11]. Table I gives the recipe for making the bio-equivalent gel phantom, and Figure 3 compares the dielectric properties of the gel phantom measured using an open-ended coaxial cable dielectric probe (SPEAG, DAK-12) and the human muscle's dielectric properties given in a database based on the measurement performed by Gabriel [12]. As can be seen from Fig. 3, the relative permittivity values of the gel phantom are close to those of the muscle, although they are lower at frequencies smaller than tens of MHz. By adjusting the ratio of various materials, we can obtain a good agreement of permittivity at some specified frequency. The same tendency can also be observed with regard to conductivity. However, covering a wide frequency range of the dielectric properties by just using one phantom is not easy; hence, we apply a correction for offsetting this influence, as shown in the following section.

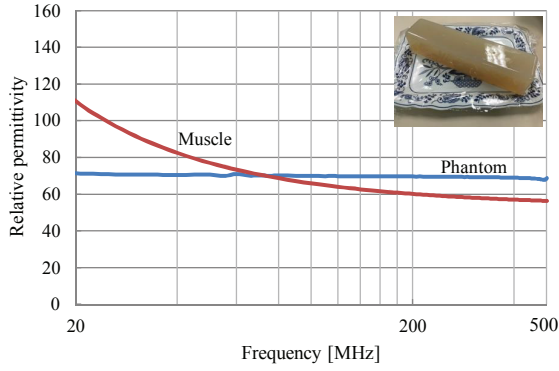


Fig. 3. Comparison of dielectric constant values between the bio-equivalent phantom and the human muscle.

### C. Bio-Signal Acquisition by Wearable Sensing Device

On the bio-equivalent phantom surface, at least one pair of sensing electrodes is set to acquire the bio-signal added to the input electrodes that are inside the phantom. This means that the bio-signal acquired on the phantom surface is different from the bio-signal added to the input electrodes, i.e., the output from the pseudo bio-signal generator, because of the existence of the bio-equivalent phantom material between the input electrodes and the sensing electrodes. Therefore, the bio-signal at the input electrodes will be distorted when it passes through the phantom material to the sensing electrodes. Then the transfer function between the output of the bio-signal generator, and the bio-signal acquired by the sensing electrodes can be expressed as  $H(j\omega)$  in the frequency domain. Therefore, to make the pseudo bio-signal acquired at the sensing electrodes be the same as the real bio-signal  $v_{real}(t)$ , we should output a pseudo bio-signal  $v_{gen}(t)$  from the generator and add it at the input electrodes as

$$v_{gen}(t) = F^{-1} \left[ \frac{V_{real}(j\omega)}{H(j\omega)}, \right] \quad (1)$$

where  $V_{real}(j\omega)$  is the Fourier transform of  $v_{real}(t)$ , and  $F^{-1}$  denotes the inverse Fourier transform. That is to say, the pseudo bio-signal generator should be designed to output  $v_{gen}(t)$ . In that case, according to Eq. (1), the signal acquired at the sensing electrodes will be identical to the real bio-signal. For deriving the transfer function  $H(j\omega)$ , we can employ a known bio-signal  $v_{known}(t)$  as the output of the bio-signal generator, and measure the signal  $v_{acqu}(t)$  acquired at the sensing electrodes on the bio-equivalent phantom surface. Then we can derive  $H(j\omega)$  as

$$H(j\omega) = \frac{F[v_{acqu}(t)]}{F[v_{known}(t)]} \quad (2)$$

where  $F$  denotes the Fourier transform. The validity of the bio-signals generated in such a way by the pseudo bio-signal generator was verified for three types of myoelectric signals.

Figure 4 shows the view of measurement setup for the three types of myoelectric signals on a human arm. The three types of myoelectric signals are from the flexor digitorum superficialis muscle, extensor digitorum muscle, and long

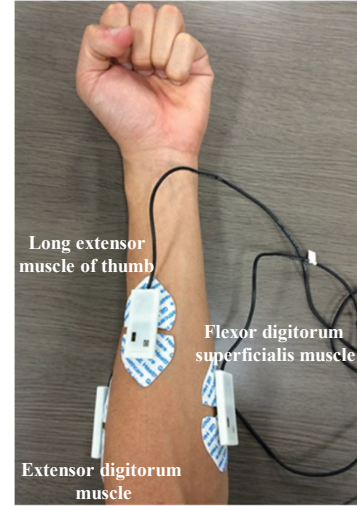


Fig. 4. View of myoelectric signal measurement setup on a human arm.

TABLE II  
CORRELATION COEFFICIENTS BETWEEN PSEUDO MYOELECTRIC SIGNALS AND REAL MYOELECTRIC SIGNALS

Muscle type	Correlation coefficients	
	w/ correction	w/o correction
Flexor digitorum superficialis muscle	0.99	0.69
Extensor digitorum muscle	0.87	0.72
Long extensor muscle of thumb	0.88	0.67

extensor muscle of the thumb, respectively. Figure 5 shows the view of acquiring the pseudo myoelectric signal through the pseudo bio-signal generator and a bio-equivalent gel phantom. Figure 6 compares the three pseudo myoelectric signals and real myoelectric signals obtained, and Table II gives the Pearson's correlation coefficients between the acquired pseudo bio-signals and the real ones. The sampling number for each signal is more than 6,000. As can be seen from Fig. 6, the pseudo myoelectric signals agree well with the real myoelectric signals. The root-mean-squared errors (RMSEs) between the pseudo signals and the real signals are 0.32 V for the flexor digitorum superficialis muscle, 0.07 V for the extensor digitorum muscle, and 0.06 V for the long extensor muscle of the thumb, respectively. The correlation coefficients are as high as 0.87 or more, as seen in Table II. For each type of myoelectric signals with correction in Table II, a P-value or probability value analysis was also performed. The p-value is the probability for a given statistical model to judge whether the null hypothesis is true. The results gave a P-value of 0.00 for all the three types of myoelectric signals, ensuring the validity of the high correlation coefficients. However, if we do not employ the correction based on Eqs. (1) and (2), the output of the pseudo bio-signal generator will differ from the signal acquired at the bio-equivalent phantom surface, and hence the correction coefficients will be poor. These are also shown in Table II for comparison. Therefore, the developed pseudo bio-signal generator together with the bio-equivalent gel phantom is usable to simulate a wearable sensing device scenario in an immunity test.

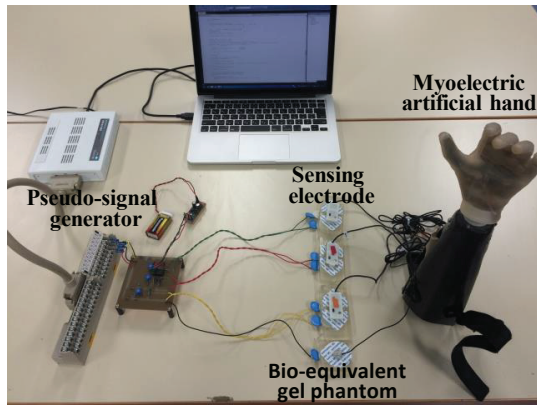


Fig. 5. View of pseudo myoelectric signal measurement setup through a bio-equivalent gel phantom.

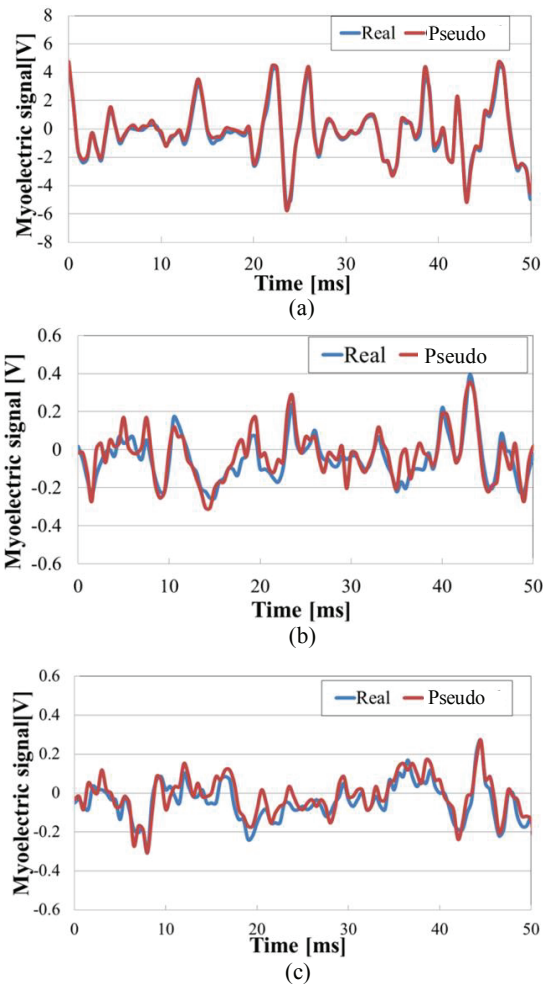


Fig. 6. Comparison of generated pseudo myoelectric signals and real myoelectric signals. (a) Flexor digitorum superficialis muscle. (b) Extensor digitorum muscle. (c) Long extensor muscle of the thumb.

### III. APPLICATION TO INDIRECT ESD TEST OF MYOELECTRIC ARTIFICIAL HAND

To demonstrate the usefulness of the developed immunity test system, we applied it to an indirect ESD test for a

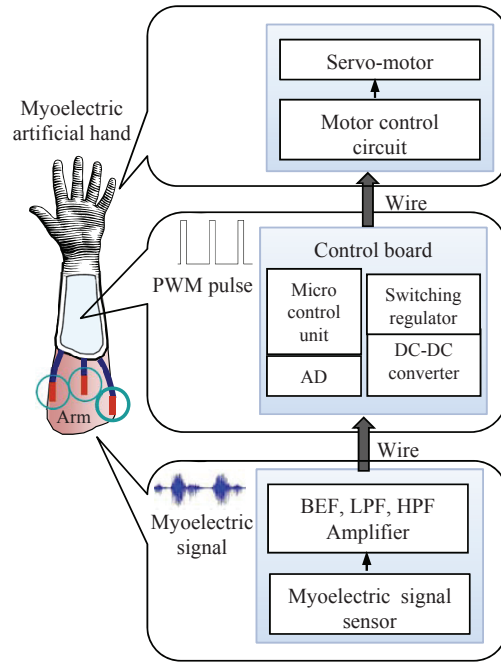


Fig. 7. Block diagram of a myoelectric artificial hand.

myoelectric artificial hand. Figure 7 shows the block diagram of the myoelectric artificial hand [13]. In this myoelectric artificial hand, the myoelectric signals in the order of mV are acquired by three pairs of sensing electrodes on the arm. They are first filtered by a 50/60 Hz band-elimination filter (BEF) as well as a low-pass filter (LPF) and a high-pass filter (HPF) respectively, and then amplified and sent to a small size control board. The micro control unit in the control board analyzes the myoelectric signals and produces the corresponding pulse width modulation (PWM) signals. The PWM signals are sent to a motor control unit at the hand for driving the servo-motors to make the artificial hand work.

#### A. Indirect ESD Test Setup and Induced ESD Noise

The IEC specifies an indirect ESD test method for electronic equipment in the IEC 61000-4-2 standard [9]. However, an immunity testing method for wearable devices attached to a human body has not been defined. Using the pseudo bio-signal generator together with the bio-equivalent gel phantom, we can conduct an indirect ESD test based on IEC 61000-4-2 without the need for a real human body.

Figure 8 shows the indirect ESD test setup and arrangement of the myoelectric artificial hand. The test setup consists of an ESD gun, a vertical coupling plane (VCP), and a horizontal coupling plane. The myoelectric artificial hand to be tested was placed at a distance of 0.1 m from the VCP and the signal line connecting the sensing electrode and the artificial hand was arranged to be perpendicular to the VCP. In the scenario with a real human body as in Fig. 8(a), the human stood at a position facing the VCP and the sensing electrodes were placed on the human arm, at a distance of 0.7 m from the VCP. Similarly, in the proposed test system of Fig. 8(b),

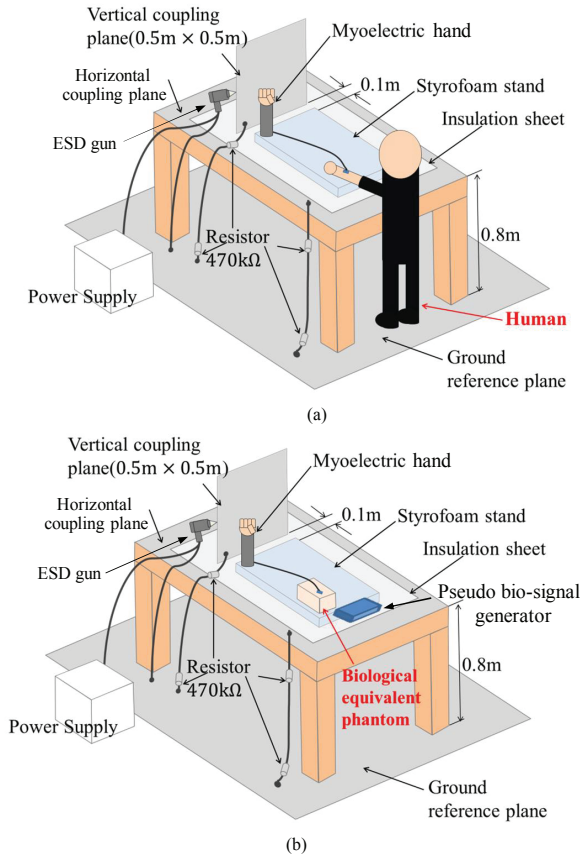


Fig. 8. Indirect ESD test setup. (a) With human body. (b) With proposed pseudo bio-signal generator and bio-equivalent gel phantom.

the bio-equivalent gel phantom was placed at a distance of 0.7 m from the VCP, and the sensing electrodes were attached on its surface.

The indirect ESD test was performed in the VCP case. First, we compared the ESD noises induced at a signal line for sending the control signal to the driving motor of the artificial hand. If the developed immunity test system consisting of the pseudo bio-signal generator and bio-equivalent gel phantom simulates the scenario of a real human body, the induced ESD noises at the control signal line should be almost the same in the two scenarios. Figure 9 shows the view of the measurement setup, and Figure 10 shows the measured ESD noise waveforms observed at the control signal line and their frequency spectra. The ESD gun's charge voltage was set to 2 kV, one of the ESD test specification levels. In the scenario with the human body, the hand was not moved so that the myoelectric signal was too weak to be observed, while in the scenario with the developed immunity test system, the ESD noise measurement was conducted without the pseudo bio-signal generator working. The induced ESD noise was measured using an isotropic photo-voltage probe (Seikoh Giken: SH-03EX) and a digital oscilloscope with a sampling frequency of 8 GHz and a frequency band of 1.5 GHz. The photo-voltage probe employs an optical fiber in place of metal wire so that no noise can be easily injected by the wiring of the probe. Moreover, due to the probe's high impedance,

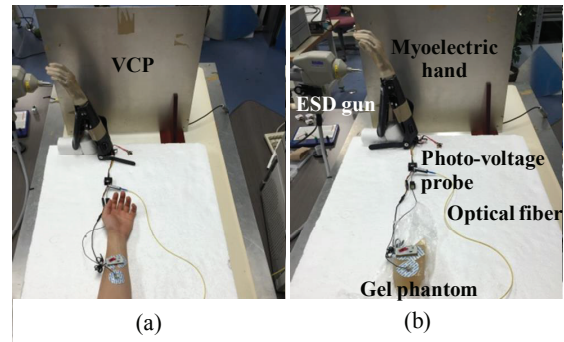


Fig. 9. View of measurement setup for ESD noises induced at the control signal line. (a) With human body. (b) With developed pseudo bio-signal generator and bio-equivalent gel phantom.

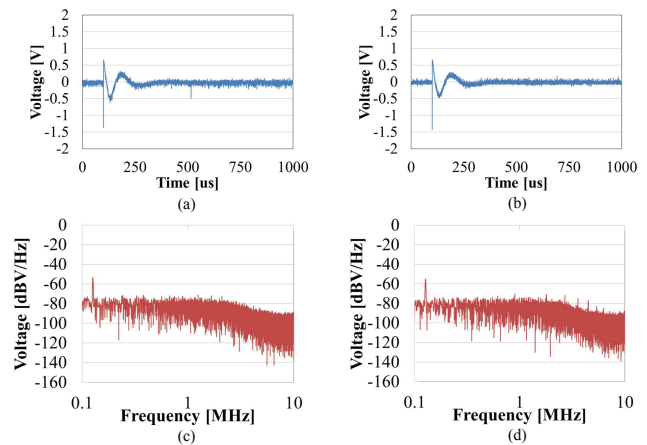


Fig. 10. Measured ESD noise at the control signal line. (a) Time waveform in the scenario with human body. (b) Time waveform in the scenario with bio-equivalent gel phantom. (c) Frequency spectrum for (a). (d) Frequency spectrum for (b).

the influence of the probe itself on the measured voltage is negligible. The photo-voltage probe has a working frequency from 100 kHz to 2 GHz, suggesting a rise time of 0.175 ns. Therefore, measuring ESD noises with a rise time of usually around 0.8 ns is sufficient.

As can be seen from Fig. 10, in both the human body and the bio-equivalent gel phantom scenarios, the induced noise waveforms were highly similar. In both scenarios, the peak values were observed as 0.6 V for positive voltage and -1.5 V for negative voltage, and the time periods from the pulse rise to convergence were approximately 200  $\mu$ s. The correlation coefficient between the two noise waveforms obtained was as high as 0.83. Next, from the frequency spectra shown in Figs. 10(c) and (d), a high similarity between the scenarios can be observed again. The noise levels were approximately -70 dBV/Hz at frequencies less than 3 MHz. The noise component of approximately -50 dBV/Hz at 125 kHz is the operating frequency noise of the switching circuit in the controller of the photo-voltage probe.

The above result indicates that the developed immunity test system is able to provide a similar ESD noise superimposed on the myoelectric artificial hand under test. This suggests that

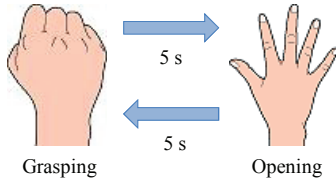


Fig. 11. Method of operation of the myoelectric artificial hand.

the immunity test result with this system should be basically equivalent to the scenario with the actual human body.

### B. ESD Test Results for Myoelectric Artificial Hand

Based on the above validation result, we tested the operation of the myoelectric artificial hand under indirect ESD conditions, according to IEC 61000-4-2, and compared the tendency of the malfunction rates in the two scenarios with the human body and the developed test system. The test layout is shown in Fig. 8, and the test conditions are listed in Table III. The ESD gun's charging voltage was changed from 1 kV to 8 kV, and the voltage polarity was either positive or negative. The discharge was repeated 999 times with an interval of 0.05 s in each test, and such a test was conducted five times under each test condition. The operation mode of the myoelectric artificial hand was set to repeat grasping and opening the hand at intervals of 5 s. This is shown in Fig. 11. During the discharge performed 999 times for each test, the operation of grasping and opening the hand was repeated continuously. The capability of the artificial hand to perform "grasping to opening" or "opening to grasping" without any difficulty during the test was employed as the performance criterion. For example, the case where the myoelectric artificial hand is able to move from "grasping to opening" but is unable to move from "opening to grasping" is decided as a malfunction or lack of immunity. In addition, in the scenario with the human body, we employed four human subjects for offsetting the influence of individual differences. With the developed test system, we measured the myoelectric signals of the four subjects using an oscilloscope and re-generated the measured signal of each subject using the pseudo bio-signal generator.

From the viewpoint of immunity, it is desirable that the developed test system provides the same or a more stringent test result as that in the human body scenario. Therefore, we also conducted the tests when the pseudo bio-signal level was changed to 0.5 and 0.75 relative to the normal myoelectric signal level. The malfunction rate was calculated from the total test results of the four subjects, i.e., the malfunction rate is the ratio of the sum of the number of malfunctions by all subjects to the total number of movements. The total number of movements was 40.

Figure 12 shows the measured malfunction rate against the ESD-gun charging voltage. Since the malfunction rate was nearly 100% when the charging voltage was 4 kV or larger, we only plotted the test results up to 3 kV in Fig. 12. The malfunction rate is found to increase in proportion to the charging voltage of the ESD gun. The malfunction mainly contained two cases. One was that the hand could

TABLE III  
ESD TEST CONDITIONS

Equipment under test (EUT)	Myoelectric artificial hand
Operating mode of EUT	Repeat grasping and opening hand
Discharge method	Contact discharge
ESD-gun coupling method	VCP
Test level	1–8 kV
Polarity	Positive, Negative
Time interval of discharge	0.05 s
Number of discharge	999

TABLE IV  
COMPARISON OF ESD POLARITY ON MALFUNCTION

Charging voltage	Positive	Negative
0 kV	1	1
2 kV	1	1
4 kV	2	2
6 kV	2	2
8 kV	2	3

1: Normal, 2: partial malfunction, 3: Complete malfunction.

not be kept in the state of "grasping" or "opening." The other was that the movement from "grasping to opening" or "opening to grasping" could not be normally performed. With the increase of the charging voltage, the latter case became more remarkable. A major cause of malfunctions was the superimposition of the ESD noise on the myoelectric signal. The myoelectric signal superimposed with the ESD noise was input to the A/D converter of the micro control unit that identifies the operation of the artificial hand, and the desired operation was erroneously identified. Another cause of malfunction was due to the superimposed ESD noise on the PWM control signal that controls the motor used to drive the artificial hand. The superimposed ESD noise influenced the PWM cycle and the duty ratio, and consequently resulted in the motor's malfunction. The immunity test system is helpful to investigate the cause of malfunction. For example, the myoelectric artificial hand used in this test had a function to confirm the movement identified by the acquired myoelectric signal on a tablet terminal. Since the tablet showed that the signal to identify an operation was different from the desired operation when a malfunction occurred during the immunity test, we can conclude that the former cause of malfunction should be more dominative.

In addition, by using the immunity test system, it is possible to investigate the coupling route of the external electromagnetic field into the wearable devices and the mechanism of their malfunction in the absence of an actual human body. For example, the myoelectric hand shown in Fig. 7 consists of three parts: the sensing part, the control board, and the motor controller. To find which part is weak in the indirect ESD test, we can shield the other two parts and perform the immunity test to see whether the unshielded part will malfunction. This is helpful to identify the coupling route of ESD noise to the artificial hand. Moreover, the immunity test system can also provide the test result of the myoelectric artificial hand for ESD polarity in the absence of an actual human body. Table IV gives the result obtained by using the developed

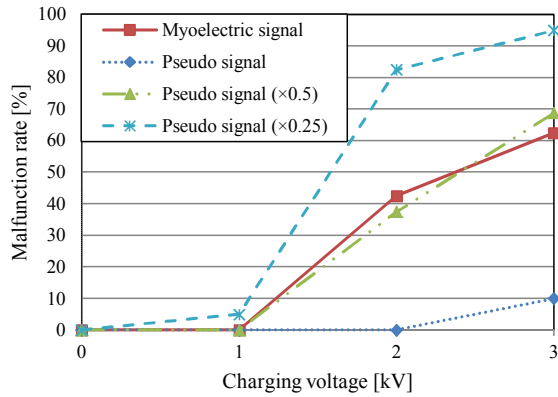


Fig. 12. Malfunction rate of myoelectric artificial hand versus ESD charge voltage.

immunity test system. Differently from Fig. 12 in which we classified the immunity test results as whether or not the artificial hand malfunctions, here we further classify the cases of malfunctions in more detail and categorized them as “partial malfunction” and “complete malfunction.” Partial malfunction means that the artificial hand did not act as specified, while complete malfunction means that the artificial hand did not have any response during the entire testing period. From Table IV, we observe that negative polarity causes a malfunction more easily. This may be because the PWM pulse used to drive the motor was split into two or more pulses by ESD noise injection [6].

As for the malfunction rate, a difference exists between the human body and the developed test system with the pseudo bio-signal generator and the bio-equivalent gel phantom. The developed test system was less susceptible to the ESD noise, and exhibited a lower malfunction rate than the scenario with human body. This difference may be attributed to the difficulty of always producing the same myoelectric signal in the real human body scenario. The actual myoelectric signal from the human arm is somewhat different every time, even for the same movement of hand, and thus it is more susceptible compared to the pseudo bio-signal, which is always output in the same and stable form. Moreover, although the ESD noise waveforms showed a high similarity between the human body and the developed test system in Fig. 10, the frequency components below 100 kHz were actually unclear due to the limitation of the photo-voltage probe, and a possibility of difference in the ESD noise component below 100 kHz may exist. However, as the pseudo bio-signal was attenuated, the malfunction rate increased. When the pseudo bio-signal level was set to 0.5 times relative to the normal level, the malfunction rate showed almost the same tendency as the human body scenario. When it was set to 0.25 times relative to the normal level, a higher malfunction rate was observed than the human body scenario. This may be used to provide a more stringent immunity test. Thus, the developed immunity system is feasible and useful to the immunity test of artificial hand with wearable myoelectric signal detectors.

### C. Discussion

As an artificial hand is usually set on the human arm and operated by myoelectric signals directly detected through the arm, it is necessary to consider the influence of the human arm and/or body on the immunity test, because there is a possibility that the human body from head to foot may play the role of a receiving antenna for the electromagnetic field. In the above indirect ESD test for the myoelectric artificial hand, the arm-sized gel phantom was found to be sufficient, because, as shown in Fig. 10, no obvious difference of measured ESD noises exists between the gel phantom and the human body scenarios. The correlation coefficient between the two noise waveforms was as high as 0.83. However, for different wearable devices, the corresponding gel phantom’s size and shape should be investigated in advance. In addition, it is difficult for a human body to always produce the same myoelectric signal. As the time of immunity test increases, the myoelectric signal may become weaker due to physical fatigue. Fig. 13 shows a measurement result of the effective (root mean square: RMS) values of myoelectric signals averaged over every one second as a function of elapsing time while the hand keeps “grasping” and “opening.” As can be seen, after 90s, the RMS value of the myoelectric signal attenuates from 1.05 V to 0.50 V in the “opening” case, and from 0.67 V to 0.33 V in the “grasping” case. This fact may be used to explain why the immunity test system provides a similar result to that of the human body when correcting the pseudo myoelectric signal to 0.5 times the actual level. Therefore, as shown in Fig. 12, introducing a correction factor of 0.5 is a reasonable choice.

It is essential to consider and define the detailed requirements for test signal specifications and the arrangement of the equipment under test (EUT) during the immunity test. Before starting the ESD test on a wearable device, it should be useful to use electric field or magnetic field probes to determine the frequency range of the radiated field. In this study, in view of the fact that the employed photo-voltage probe has a frequency range from 100 kHz to 2 GHz, the measurement result of ESD noise should be sufficiently reliable. From the measurement result shown in Fig. 10, the main frequency components are observed below 3 MHz, and they further attenuate by nearly 20 dB at 10 MHz; hence, the developed immunity test system fully covers the possible frequency range and is thus valid.

## IV. CONCLUSION

In this study, we developed an immunity test system consisting of a pseudo bio-signal generator and a bio-equivalent gel phantom that helps simulate an environment to acquire bio-signals on the human body. As an example, we used the pseudo bio-signal generator to produce three kinds of myoelectric signals and confirmed a high correlation coefficient of larger than 0.87 with actual myoelectric signals. To verify the usefulness of the developed immunity test system, we applied it to the testing of a myoelectric artificial hand for indirect ESD according to IEC 61000-4-2. We found that (1) the ESD noise superimposed on the control signal line of the artificial hand agrees with that when a human body actually exists; (2) the malfunction rate shows the same tendency as that with the

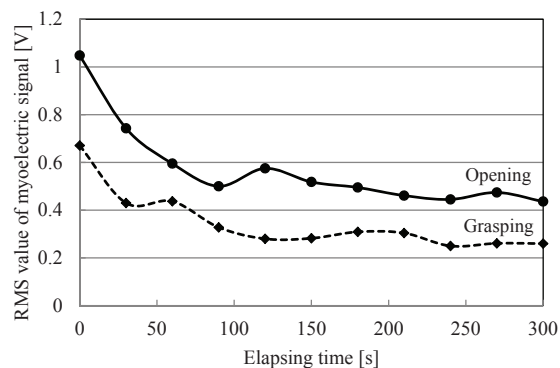


Fig. 13. RMS value of myoelectric signal (after amplifier) averaged every second as a function of elapsing time.

human body although the latter is more susceptible. From the viewpoint of immunity, the test can be conducted by adjusting the pseudo bio-signal level so that the developed test system facilitates a more stringent test. In the myoelectric artificial hand case, we found a tendency of malfunction similar to that with the human body, and when the output level of the pseudo bio-signal generator was corrected by 0.5 times, the test system could provide a very similar test result to that with the human body. Thus, the developed immunity system is sufficiently useful to the immunity test of various wearable devices.

For efficiently using the developed immunity system, detailed requirements for test signal specifications and arrangements of the EUT need to be defined. These require a detailed investigation according to the intended use of wearable devices, and will be the subject of our future research.

#### ACKNOWLEDGMENT

This study was supported partially by JSPS KAKENHI under Grant 15H04006, and the Gigabit Research Consortium of the University of Electro-Communications, Japan. The authors would like to thank Y. Murase and K. Nagai, Nagoya Institute of Technology, for their help in measurement data acquisition.

#### REFERENCES

- [1] J. Wang and Q. Wang, "Body Area Communications", Wiley-IEEE, 2012.
- [2] IEEE Standard for Local and Metropolitan Area Networks? Part 15.6: Wireless Body Area Networks, IEEE Standard 802.15.6-2012, Feb. 2012.
- [3] P. Bonato, "Wearable sensors and systems - From enabling technology to clinical applications", IEEE Eng. Med. Biol. Mag., vol. 29, no. 3, pp. 25-36, May/June. 2010.
- [4] E. Nemati, M. J. Deen and T. Mondal, "A wireless wearable ECG sensor for long-term applications," IEEE Commun. Mag., vol. 50, no. 1, pp. 36-43, Jan. 2012.
- [5] T. Ishida, S. Nitta, F. Xiao, Y. Kami and O. Fujiwara, "An experimental study of electrostatic discharge immunity testing for wearable devices", Proc. Joint IEEE Int. Symp. on EMC & EMC Europe, Dresden, Germany, pp. 839-842, Aug. 2015
- [6] C. Ji, D. Anzai, J. Wang, I. Mori and O. Fujiwara, "An ESD immunity test for battery-operated control circuit board in myoelectric artificial hand system", IEICE Trans. Commun., vol. E98-B, no. 12, pp. 2477-2484, Dec. 2015.

- [7] W. Liao, J. Shi and J. Wang, "An approach to evaluate electromagnetic interference with wearable ECG at frequencies below 1 MHz", IEICE Trans. Commun., vol. E98-B, no.8, pp.1606-1613, Aug. 2015.
- [8] W. Liao, J. Shi and J. Wang, "Electromagnetic interference of wireless power transfer system on wearable electrocardiogram", IET Microwaves, Antennas & Propagation, vol. 11, no. 3, pp. 330-335, April 2017.
- [9] International Electrotechnical Commission, IEC 61000-4-2, Edition 2.0, Dec. 2008.
- [10] J. Wang, D. Anzai, O. Fujiwara, Y. Kami, T. Ishida and F. Amemiya, "A report of ESD immunity testing relating to body worn equipment using robotic technology including electro-technology", CISPR/I/WG4 Contribution, 17-01, Feb. 2017.
- [11] K. Ito, H. Kawai and K. Saito, "State of the art and future prospects of biological tissue-equivalent phantoms", Trans. IEICE, vol. B85, no.5, pp. 582-596, May 2002.
- [12] C. Gabriel, "Compilation of the dielectric properties of body tissues at RF and microwave frequencies", Brooks Air Force, San Antonio, TX, AL/OE-TR-1996/0037, 1996.
- [13] T. Seki, T. Nakamura, R. Kato, S. Morishita and H. Yokoi, "Development of five-finger multi-DoF myoelectric hands with a power allocation mechanism", Journal of Mechanics Eng. and Automation, vol.4, pp.97-105, 2014.



electromagnetic compatibility.

**Jianqing Wang** (M'99) received the B.E. degree in electronic engineering from Beijing Institute of Technology, Beijing, China, in 1984, and the M.E. and D.E. degrees in electrical and communication engineering from Tohoku University, Sendai, Japan, in 1988 and 1991, respectively. He was a Research Associate at Tohoku University and a Senior Engineer at Sophia Systems Co., Ltd., prior to joining the Nagoya Institute of Technology, Nagoya, Japan, in 1997, where he is currently a Professor. His research interests include biomedical communications and



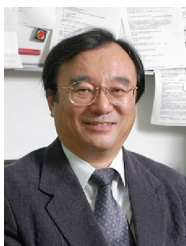
**Ryo Nakaya** received the B.E. and M.E degrees in electrical and electronic engineering from Nagoya Institute of Technology, Nagoya, Japan, in 2015 and 2017, respectively. During he was a graduate student at Nagoya Institute of Technology, he was involved in the development of immunity test system for wearable devices. He is currently with Toyota Industries Corporation, Japan.



**Keisuke Sato** received the B.E. and M.E degrees in electrical and electronic engineering from Nagoya Institute of Technology, Nagoya, Japan, in 2014 and 2016, respectively. During he was a graduate student at Nagoya Institute of Technology, he was involved in the development of immunity test system for wearable devices. He is currently with Konica Minolta, Inc., Japan.



**Daisuke Anzai** (S'06-M'11) received the B.E., M.E. and Ph.D. degrees from Osaka City University, Osaka, Japan in 2006, 2008 and 2011, respectively. Since April 2011, he has been an Assistant Professor at the Graduate School of Engineering, Nagoya Institute of Technology, Nagoya, Japan. He has engaged in the research of biomedical communication systems and localization systems in wireless communication networks.



**Osamu Fujiwara** (M'84-LM'13) received his B.E. degree in electronic engineering from the Nagoya Institute of Technology, Nagoya, Japan, in 1971, and his M.E. and D.E. degrees from Nagoya University, Nagoya, Japan, in 1973 and 1980, respectively, both in electrical engineering. From 1973 to 1976, he was with the Central Research Laboratory, Hitachi Ltd., Kokubunji, Japan, where he was engaged in research and development of system packaging designs for computers. From 1980 to 1984, he was with the Department of Electrical Engineering, Nagoya University,

as a Research Associate, and from 1984 to 1985, as an Assistant Professor. In 1985, he joined the Nagoya Institute of Technology, as an Associate Professor. In 1993, he became a Professor with the Graduate School of Engineering, Nagoya Institute of Technology. In 2012, he retired and was awarded Emeritus Professor from National University Corporation, Nagoya Institute of Technology. His research interests include bioelectromagnetics and electromagnetic compatibility.



**Fujio Amemiya** (M'08) received the B.E., M.E., and Dr. Eng. degrees in communication engineering from Tohoku University, Sendai, Japan, in 1997, 1993, and 2007, respectively. In 1973, he joined the Musashino Electrical Communication Laboratories, Nippon Telegraph and Telephone Republic Corporation (now NTT), Tokyo, Japan. He is currently an Engineer at NTT Advanced Technology Corporation. Since 2015, he has also been a Guest Professor at Organization for Research Promotion Center for Industrial and Governmental Relations,

The University of Electro-Communications. He has been involved in developmental research on electric and digital telephone sets. Since 1988, he has been involved in research and development of the EMC for telecommunication equipment and systems. He is also the Technical Secretary of IEC CISPR Subcommittee I.